COMPARISON OF AERIAL IMAGERY FROM MANNED AND UNMANNED AIRCRAFT PLATFORMS FOR MONITORING COTTON GROWTH

Chenghai Yang
USDA-ARS
College Station, TX
Juan Landivar
Murilo Maeda
Texas AgriLife Research and Extension Center
Corpus Christi, TX
Jinha Jung
Michael J. Starek
Tianxing Chu
Anjin Chang
Texas A&M University
Corpus Christi, TX

Abstract

Unmanned aircraft systems (UAS) have emerged as a low-cost and versatile remote sensing platform in recent years, but little work has been done on comparing imagery from manned and unmanned platforms for crop assessment. The objective of this study was to compare imagery taken from multiple cameras on manned and unmanned aircraft platforms for monitoring cotton growth. A manned aircraft equipped with a red-green-blue (RGB) camera, a modified near infrared (NIR) camera, a thermal camera and a hyperspectral camera was used to take images from test plots. Two rotary wing UAS equipped with a RGB camera and a modified color-infrared (CIR) camera, respectively, and a fixed wing UAS equipped with a different modified CIR camera were used to acquire high-resolution images from the plots. The RGB/NIR/CIR imagery taken by both the manned and unmanned platforms on June 23, 2016 was used. The RGB/NIR/CIR images from all the platforms were registered to each other and the images from the unmanned platforms were aggregated and resampled to the coarser resolution in the imagery from the manned platform. Correlation coefficients were calculated among all the visible and NIR bands. Normalized difference vegetation index (NDVI) images were also calculated from all the CIR images. Comparison of the RGB images from the manned and unmanned platforms revealed that some subtle color differences between cotton genotypes could have been smoothed out in the mosaicked UAS imagery possibly due to color balancing. Correlation analysis showed that the visible bands in the RGB imagery and the NIR band in the CIR imagery from the unmanned platforms were positively related to the respective bands in the RGB and NIR imagery from the manned platform. However, the red and green bands in the CIR imagery from the UAS platforms were poorly related to the respective bands in the RGB imagery from the manned platform. The preliminary results from this study indicate that the modified CIR cameras may not have appropriate spectral response in the visible bands and some useful spectral differences may have been smoothed out in mosaicked UAS imagery.

Introduction

Unmanned aircraft systems (UAS) are being increasingly used as a remote sensing platform to acquire high spatial resolution imagery due to their low cost, low flight altitude, and high revisit frequency. These systems fill a gap between manned and ground-based platforms and they have been used for diverse agricultural applications (Whitehead and Hugenholtz, 2014). There are two types of UAS platforms, fixed-wing and rotary-wing, and each can carry various types of remote sensing sensors. Fixed-wing UAS typically have longer ranges and higher speeds, while rotary-wing UAS offer greater maneuverability. Due to their payload limitations, most UAS platforms are equipped with low-cost and lightweight cameras, including modified consumer-grade cameras. Several companies offer such cameras that are able to capture color-infrared (CIR) imagery with one single sensor, but limited information is available on the performance of this type of cameras.

Under the current small UAS rule in the U.S., UAS can fly no more than 400 ft above ground level (AGL). The low-flying height is a benefit for some remote sensing applications that require very high-resolution image data, such as for plant counting and plant height estimation (Chu et al., 2016). However, the low flying height restricts ground area coverage. Consequently, a large number of images need to be collected with very high overlaps (70-85%) to cover the area of interest and enable sufficient feature correspondence during the structure-from-motion photogrammetric processing commonly applied to UAS image sequences. Then the individual images collected over a certain time with varying degrees of geometric distortion and radiometric variation need to be mosaicked as a seamless image. Platform stability, change in lighting conditions during image acquisition, forward and side overlaps, and image mosaicking can all introduce errors to the final mosaicked image. As UAS are gaining popularity, it is necessary to evaluate the performance of the low-cost cameras used in UAS and to assess the quality of the final mosaicked image. The objective of this study was to compare imagery taken from multiple cameras mounted on manned and unmanned aircraft platforms for monitoring cotton growth.

Materials and Methods

Study Site

This research was conducted in a 1000-ft x 5000-ft experimental area at the Texas AgriLife Research and Extension Center in Corpus Christi, Texas. A 500-ft x 700-ft area with the center coordinates (27°46'57"N, 97°33'39"W) within the experimental area was selected for this study. Thirty-one cotton genotypes were planted in the small study area in two-row plots that were 33 ft. long and had a row spacing of 38 in.

Manned Aircraft and Cameras

A Cessna 206 aircraft, equipped with three imaging systems (multispectral, hyperspectral and thermal), was used as the manned platform for image acquisition. The multispectral imaging system consisted of two Nikon D810 digital cameras with a 7360 × 4912 pixel array. One camera captured normal RGB color images, while the other camera was equipped with an 830-nm long band-pass filter to obtain NIR images. The hyperspectral imaging system consisted of a Headwall Hyperspec imaging spectrometer and a GPS/inertia navigation system. The spectrometer could capture 16-bit hyperspectral images with a swath of 1608 pixels and 120 spectral bands in the 400-1000 nm spectral range. The thermal camera was a FLIR model SC640 camera sensitive in the 7.5 to 13 µm spectral range to capture 14-bit thermal images with a 640 × 480 pixel array. The RGB and NIR images from Nikon D810 cameras were used in this paper.

Unmanned Aircraft and Cameras

Two rotary-wing and one fixed-wing UAS were used as the unmanned platforms. A DJI Phantom 4 multirotor UAS equipped with a FC330 RGB camera was used to capture RGB imagery. The camera was configured to capture 8-bit RGB imagery with a 2000 × 1500 pixel array. A 3DR X8+ multirotor UAS equipped with a Tetracam ADC Snap camera was used to take CIR imagery. The camera captured 10-bit NIR-R-G imagery with 1280 × 1024 pixels. A senseFly eBee fixed wing UAS equipped with a Canon S110 camera was also used to capture CIR imagery. The camera obtained R-G-NIR imagery with 4048 × 3048 pixels.

Image Acquisition

Airborne RGB and NIR imagery from the manned platform was acquired at 305 m (1000 ft.) AGL between 1200 and 1500h local time under sunny conditions on June 10, 23, July 7 and August 3, 2016. UAS imagery was acquired from the DJI Phantom 4 at 20 m (66 ft) AGL, the 3DR X8+ at 50 m (164 ft) AGL, and the Sensefly eBee at 103 m (338 ft) AGL every week during the growing season. The imagery collected from all four platforms on June 23 was used for analysis. The camera and image parameters for the platforms are summarized in Table 1.

Table 1. Camera and image parameters for a manned and three unmanned aircraft platforms

Platform	Camera	Image	Pixel Array	Pixel Depth (bit)	Flight Height (m)	Pixel Size (cm)
Cessna 206	Two Nikon D810	R-G-B, 3 NIR	7360×4912	14	305	9
DJI Phantom 4	FC330	R-G-B	2000×1500	8	20	0.9
3DR X8+	Tetracam ADC Snap	NIR-R-G	1280×1024	10	50	2.4
senseFly eBee	Canon S110	R-G-NIR	4048×3048	16	100	4.0

Image Analysis

The RGB and NIR images from the two Nikon D810 cameras were align using an image-to-image registration procedure based on the first-order polynomial transformation model and then stacked as a six-band image. As the three NIR bands from the modified D810 NIR camera were similar, the NIR band image recorded in the green channel was used to create the CIR composite image along with the red and green bands in the RGB image. Among all the images, the FC330 image had the highest spatial resolution, so the other images were registered to it. Then all the images were rectified to the Universal Transverse Mercator (UTM), World Geodetic System 1984 (WGS-84), Zone 14, coordinate system based on a set of ground control points in the study area. Since the UAS images had finer spatial resolutions, they were aggregated and resampled to the 9-cm coarser spatial resolution of the D810 image. Normalized difference vegetation index (NDVI) images were generated for the D810 CIR image and the two UAS CIR images. Correlation coefficients among all the bands and the three NDVIs were calculated. All procedures for image registration and analysis were performed using ERDAS Imagine (Intergraph Corporation, Madison, AL).

Results and Discussion

Figure 1 shows the RGB image from the Nikon D810 camera on the manned aircraft and the mosaicked RGB image from the FC330 camera on the DJI Phantom 4 UAS. The FC330 image looked similar to the D810 image, though they had slightly different color tones. A close visual examination of the images revealed that some of the cotton genotypes had a lighter green tone, especially on the D810 image.

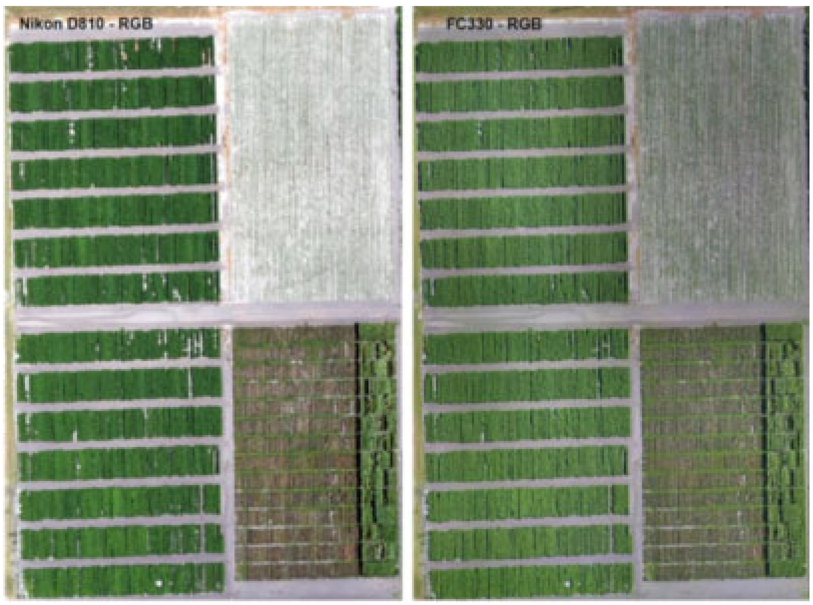

Figure 1. RGB image from a Nikon D810 camera on a manned aircraft (left) and mosaicked RGB image from a FC330 camera on a DJI Phantom 4 UAS (right).

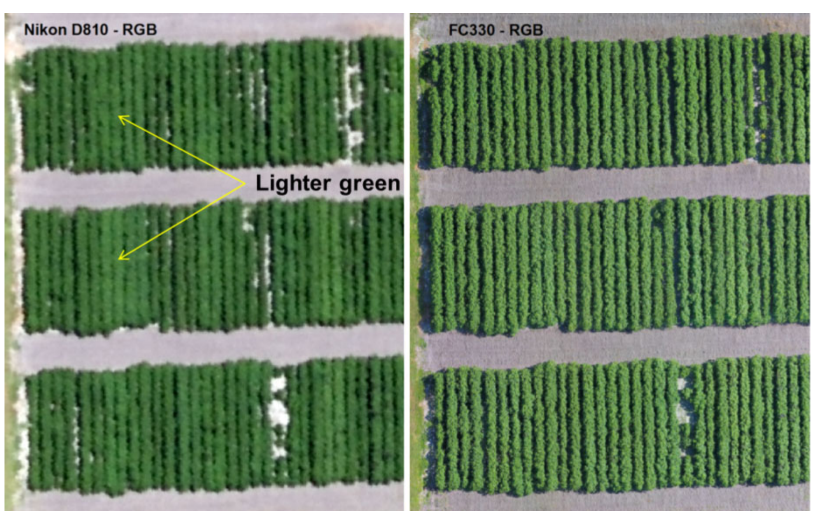

Figure 2. Upper-left portion of the RGB images shown in Figure 1 from a Nikon D810 camera on a manned aircraft (left) and from a FC330 camera on DJI Phantom 4 UAS (right).

Figure 2 shows the upper-left portion of the RGB images. Some of the rows on the D810 image had a lighter green tone, but such a color difference was hardly visible on the FC330 image. Since the D810 image was captured instantaneously, all the pixels in the image maintained their spatial and spectral integrity. In contrast, the FC330 image was a mosaic of hundreds of images that were captured at different times with varying degrees of geometric distortions and radiometric variations. Some of the subtle color differences could have been smoothed out by color balancing and averaging during the image mosaicking process. Other factors such as camera types and settings could have also contributed to the difference.

Figure 3 shows the CIR image from the manned aircraft and two mosaicked CIR images from the UAS platforms. The CIR image from the D810 cameras had the typical color tones with plants appearing reddish and bare soil cyanish. However, the two CIR image mosaics from the Tetracam ADC Snap camera and the Canon S110 camera had different color tones, indicating the two CIR cameras may not have accurate spectral response.

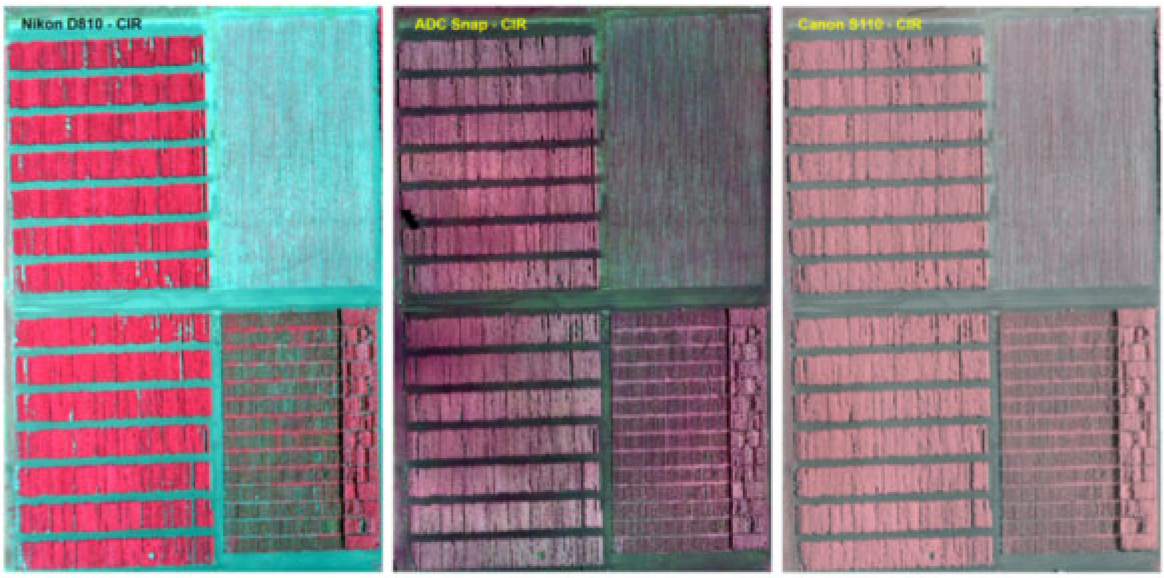

Figure 3. CIR composite image from two Nikon D810 cameras on a manned aircraft (left) and mosaicked CIR images from a Tetracam ADC Snap camera on a 3DR X8+ UAS (center) and a Canon S110 camera on a senseFly eBee UAS (right).

Table 2. Correlation matrix between 13 bands in five images from five different cameras on one manned aircraft and three UAS platforms

Platform		Manned				Unmanned								
Aircraft		Cessna 206				DJI Phantom 4			3DR X8+			senseFly eBee		
Camera		Nikon D810 RGB&NIR				FC330			Tetracam ADC Snap			Canon S110		
	Band	R	G	B	NIR	R	G	B	NIR	R	G	R	G	NIR
Nikon D810	R	1.00	**0.97**	**0.98**	**-0.56**	**0.67**	0.46	0.71	-0.38	**0.07**	-0.10	**0.31**	0.21	-0.30
	G	0.97	1.00	0.97	-0.36	0.65	**0.50**	0.68	-0.24	0.18	**0.03**	0.42	**0.34**	-0.13
	B	0.98	0.97	1.00	-0.56	0.65	0.46	**0.74**	-0.39	0.07	-0.11	0.29	0.20	-0.30
	NIR	-0.56	-0.36	-0.56	1.00	-0.38	-0.07	-0.52	**0.70**	0.32	0.48	0.30	0.40	**0.76**
FC330	R	0.67	0.65	0.65	-0.38	1.00	0.92	0.92	-0.05	0.35	0.20	0.45	0.35	-0.05
	G	0.46	0.50	0.46	-0.07	0.92	1.00	0.77	0.25	0.51	0.43	0.58	0.52	0.25
	B	0.71	0.68	0.74	-0.52	0.92	0.77	1.00	-0.26	0.21	0.02	0.28	0.17	-0.26
ADC Snap	NIR	-0.38	-0.24	-0.39	0.70	-0.05	0.25	-0.26	1.00	0.76	0.90	0.51	0.59	0.80
	R	0.07	0.18	0.07	0.32	0.35	0.51	0.21	**0.76**	1.00	0.94	0.60	0.61	0.54
	G	-0.10	0.03	-0.11	0.48	0.20	0.43	0.02	**0.90**	0.94	1.00	0.60	0.64	0.68
Canon S110	R	0.31	0.42	0.29	0.30	0.45	0.58	0.28	0.51	0.60	0.60	1.00	0.99	**0.77**
	G	0.21	0.34	0.20	0.40	0.35	0.52	0.17	0.59	0.61	0.64	0.99	1.00	**0.84**
	NIR	-0.30	-0.13	-0.30	0.76	-0.05	0.25	-0.26	0.80	0.54	0.68	0.77	0.84	1.00

Table 2 presents the correlation matrix among the 13 bands from the five cameras on the four platforms. Generally, the three visible bands are highly positively related, whereas the NIR band is negatively related with the three visible bands as shown by the correlation coefficients among the four bands in the D810 GRB and NIR images in Table 2 and by the scatterplots in Figure 4.

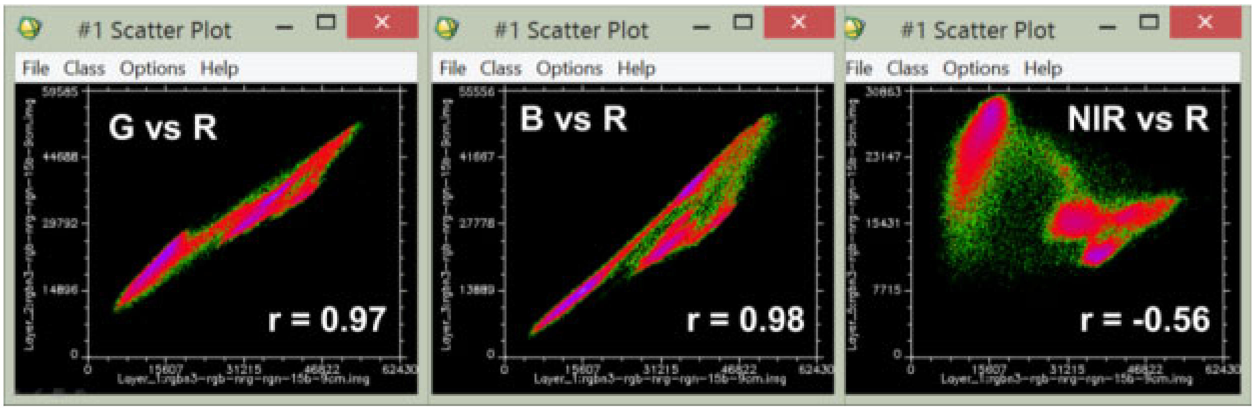

Figure 4. Scatterplots among visible and NIR bands in images from two Nikon D810 cameras on a manned aircraft.

From Table 1, the RGB bands in the D810 image were positively related to the corresponding RGB bands in the FC330 image with respective R-values of 0.67, 0.50 and 0.74, and the NIR band in the D810 was also positively related the NIR bands in the ADC Snap and S110 images with respective R-values of 0.7 and 0.76. These R-values indicated that there existed some differences in the corresponding bands among the three cameras. Moreover, much weaker correlations were found among the three red bands in the D810, ADC Snap and S110 CIR images. The same is true among the three green bands. For example, the red band in the D810 image had an R-value of 0.07 with the red band in the ADC Snap image and an R-value of 0.31 with the red band in the S110 image. The green band in the D810 CIR image had R-values of 0.03 and 0.34 with the respective green bands. These extremely low R-values, especially for the ADC Snap camera, indicated that the red and green bands in the CIR images from the Tetracam ADC Snap camera and the Canon S110 camera had obvious problems. In fact, the NIR bands were highly positively related to the respective red and green bands with R-values of 0.76 and 0.90 for the Snap image and 0.77 and 0.88 for the S110 image. As mentioned previously, the NIR band is generally negatively related to the visible bands, indicating that the red and green bands from the two CIR cameras were contaminated with NIR light.

Figure 5 shows the NIR, red and green band images in the three CIR images. The scatterplots of the bands in the D810 CIR image with the corresponding bands in the Snap and S110 CIR images are also shown in the figure. As expected, on the D810 NIR band image, lush crop plants had a light gray color, while bare soil had a dark gray tone. The contrast between plants and bare soil on the NIR band images from the two UAS CIR cameras was not as distinct, but the general color tone appeared to be correct.

On the D810 red band image, plants had a dark gray color, while bare soil had a light gray response. However, plants looked brighter than bare soil in the red band image from the Snap camera. In fact, the red band image was similar to the NIR image except that it was slightly darker. For the S110 camera, the red band image appeared flat with a very small contrast between plants and bare soil. The D810 green band image was similar to the red band image, but plants did not appear as dark because plants had higher reflectance in the green band. The green band images from the two UAS CIR cameras were also similar to their respective red band images. Clearly, the red and green bands in the ADC Snap camera and S110 camera did not have appropriate spectral response. This visual assessment agreed with the correlation analysis results.

Figure 6 presents the NDVI images derived from the three CIR images. As shown in the D810 NDVI image, lush plants had a light gray color, while bare soil had a dark gray tone. Due to the problems associated with the red bands in the Snap and S110 cameras, the NDVI images from the two cameras were not reliable. The NDVI image for the Snap camera did not appear to separate crop plants effectively. This observation was further supported by its scatterplot and low correlation coefficient (0.50) with the D810 NDVI image. Although the NDVI image from the

S110 camera had a high correlation coefficient (0.88) with the D810 NDVI image, it did not exhibit the spatial variability and details as shown in the D810 NDVI image partly due to its flat red band image.

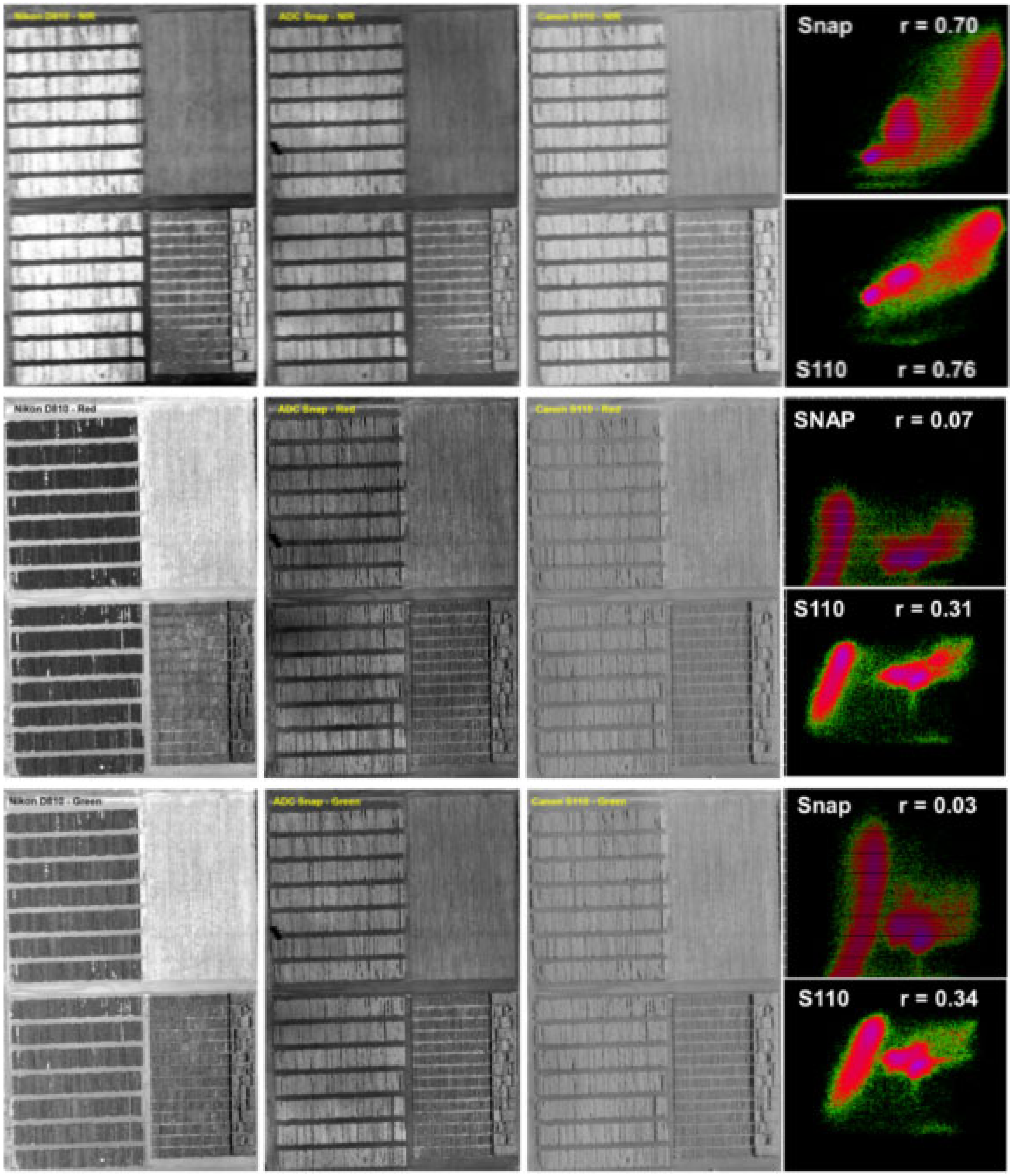

Figure 5. NIR (top row), red (middle row), and green (bottom row) band images in the CIR image from two Nikon D810 cameras on a manned aircraft (first column) and in the mosaicked CIR images from a Tetracam ADC Snap camera on a 3DR X8+ UAS (second column) and a Canon S110 camera on a senseFly eBee UAS (third column). The scatterplots of the D810 bands with the corresponding Snap and S110 bands are also shown in the figure.

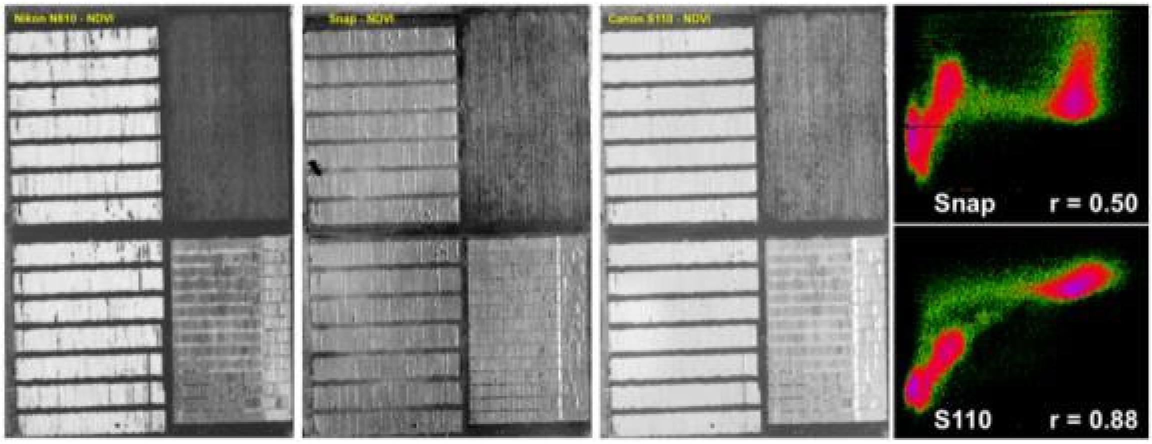

Figure 6. NDVI images from a D810 CIR image (left), a mosaicked ADC Snap CIR image (center) and a Canon S110 camera on a senseFly eBee UAS. Scatterplots of the D810 NDVI image with the Snap and S110 NDVI images are also shown in the figure.

Conclusions

This study compared imagery taken from two cameras on a manned aircraft platform and three cameras on three UAS platforms for monitoring cotton growth. Comparison of the RGB images from the manned and unmanned platforms revealed that some subtle color differences could have been smoothed out by color balancing and averaging during the image mosaicking process. Correlation analysis and visual assessment showed that the visible bands in the RGB imagery and the NIR band in the CIR imagery from the three cameras on the UAS platforms were positively related to the respective bands in the RGB and NIR imagery from the manned platform. However, the red and green bands from the two CIR cameras on the UAS were poorly related to the respective bands in the RGB imagery from the manned platform. The preliminary results from this study indicate that the two modified CIR cameras may not have appropriate spectral response. More field experiments are needed to evaluate the performance of these low-cost cameras and the effects of UAS flight parameters (height, speed, overlaps) and image mosaicking on image quality.

Acknowledgements

This project was partly funded by the Texas State Support Committee and Cotton Incorporated, Cary, NC. The authors wish to thank Fred Gomez and Lee Denham of USDA-ARS at College Station, TX for taking the aerial imagery for this study. Thanks are also extended to the UAS crew at Texas A&M University-Corpus Christi for taking the UAS imagery for this study. Mention of trade names or commercial products in this article is solely for purpose of providing specific information and does not imply recommendation or endorsement by the U.S. Department of Agriculture. USDA is an equal opportunity provider and employer.

References

Chu, T., R. Chen, J.A. Landivar, M.M. Maeda, C. Yang, and M.J. Starek. 2016. Cotton growth modeling and assessment using unmanned aircraft system visual-band imagery. Journal of Applied Remote Sensing 10(3):036018.

Whitehead, K., and C.H. Hugenholtz. 2014. Remote sensing of the environment with small unmanned aircraft systems (UASs), part 1: a review of progress and challenges. Journal of Unmanned Vehicle Systems 2(3): 69-85.